Mechanism of Roughness Profile Transfer in Skin-pass Rolling of Thin Steel Strip

KIJIMA Hideo[*1]

Abstract:

Skin-pass rolling (or temper rolling) is usually the final process in the production of cold-rolled steel sheets. One of the main objectives in skin-pass rolling is to obtain a certain surface roughness profile. In this paper, the mechanism of roughness profile transfer in skin-pass rolling is investigated by experimental rolling tests as well as numerical analysis by elastic-plastic FEM in terms of material deformation and lubrication. Roughness transfer in skin-pass rolling could be modeled as vertical indentation of the roughness profile because the peak pressure which can be estimated by Hertzian elastic contact is the most important parameter. The effect of the lubrication can be explained convincingly and reasonably by height characterization parameters. When elongation is small, the effect of lubrication is not observed in elongation and roughness transfer. After the effect of lubrication had appeared, the trapped lubricant supports pressure.

1. Introduction

Skin-pass rolling (or temper rolling) is usually the final forming step in the production of cold-rolled steel sheets, following the annealing process. In this process, mechanical properties, strip flatness, the surface roughness profile and other product properties are determined so as to satisfy customer requirements by rolling with small reduction[1, 2]. The conditions in skin-pass rolling are unique as a sheet rolling process due to the small reduction (approximately 1%), large contact length relative to the change in sheet thickness, large roll radius relative to the contact length and high friction. In addition to these characteristics, the work roll surface is intentionally roughened in some cases to achieve a required strip surface roughness. Because these conditions are quite different from those in conventional hot and cold rolling, conventional rolling theory is not appropriate for analysis of the skin-pass rolling process. To date, calculation of skin-pass rolling force was attempted based on conventional two-dimensional rolling theory[3], and a laboratory experiment was conducted with a small roll diameter of approximately100 mm[4].

It is well known that surface roughness on a steel sheet surface affects corrosion resistance, image clarity after painting and formability in press forming, including galling behavior with tools[5]. Numerous experimental studies have examined technologies for achieving a preferable roughness profile as well as surface processing technology[6, 7]. In particular, for press formability, it is important to form certain micro pockets of lubricant on the sheet surface, and for image clarity reducing waviness in the long wavelength region is considered crucial.

Recently, the Finite Element Method (FEM) has been applied to analyze skin-pass rolling conditions, taking advantage of the dramatically higher calculation capacity of computers and improved stability and reliability of commercial source codes[8–10]. Moreover, microscopic analyses considering work roll surface roughness have been conducted[11, 12], and three-dimensional analysis has also been attempted[13].

In this research, based on the basic characteristics of strip deformation and the contact condition between the strip and work roll in skin-pass rolling[10], the mechanism of the effects of roughness transfer and lubrication[12, 14, 15] is clarified, and useful knowledge for practical operation is introduced as a verified simplification. In this report, experimental and analytical approaches to the skin-pass rolling mechanism are described in relation to the characteristics of skin-pass rolling as a thin strip rolling process and roughness transfer.

† Originally published in *JFE GIHO* No. 42 (Aug. 2018), p. 57−62

[*1] Dr. Eng.,
Senior Researcher General Manager,
Rolling & Processing Research Dept.,
Steel Res. Lab.,
JFE Steel

2. FEM Analysis of Normal Pressure Distribution in Skin–Pass Rolling

2.1 Experimental and Analytical Conditions

A skin-pass rolling experiment was conducted under a dry condition with a laboratory rolling mill, which was simulated by two-dimensional plane strain FEM analysis.

In the rolling experiment, the workpiece was an annealed low carbon steel sheet which dimensions of thickness 0.69 mm, width 80 mm and length 300 mm. The work roll diameter and barrel width were 500 mm and 150 mm. This diameter is similar to that of the work rolls of operational mills. The work roll material was a high chromium steel, SUJ2, and the roll surface was ground to 0.2 μm Ra. To achieve a dry friction condition, the roll and workpiece surfaces were carefully degreased with petroleum benzine before rolling. Because a cut sheet was used, rolling tension was not applied.

Figure 1 [10] shows a schematic outline of the skin-pass rolling model. Considering symmetry, only the upper half of the workpiece and the upper roll were modeled. The roll was modeled as an elastic body having Young's modulus of 205.8 GPa and Poisson's ratio of 0.3. For ease of calculation, the central part corresponding to the half radius was modeled as rigid. The workpiece was assumed to be elastic-plastic with the same elastic properties as the work roll. The plastic properties of initial yield stress and work-hardening were determined from a tensile test. The contact problem between the work roll and the workpiece was solved by the penalty method. To simulate the dry friction condition, a friction coefficient of 0.3 was used[16]. The commercial software Abaqus Standard (v6) was used. As a comparison, simple vertical compression by a roll under the above-mentioned conditions was also analyzed. The surface roughness profiles of the work roll and workpiece were not considered.

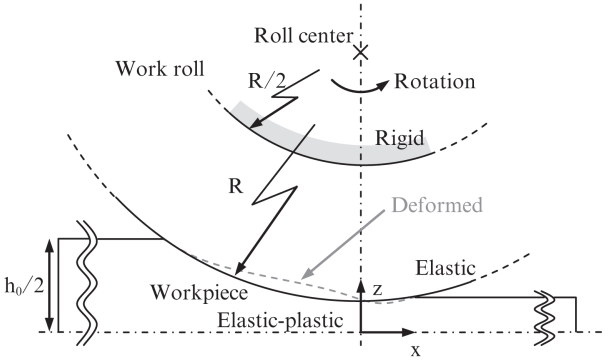

Fig. 1 Schematic outline of skin-pass rolling model[10]

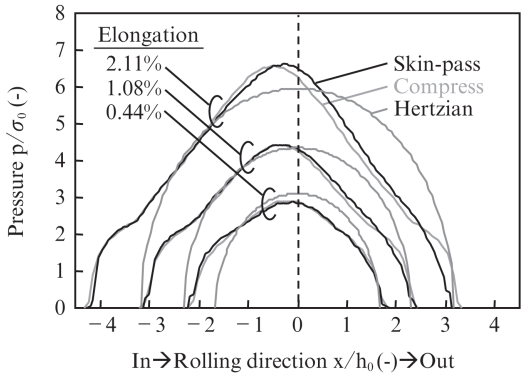

Fig. 2 Pressure distribution in skin-pass rolling, simple compression and Hertzian elastic contact[10]

2.2 Comparison of Surface Pressure Distribution in FEM Analysis

Figure 2 [10] shows the calculated pressure distribution for skin-pass rolling and simple compression as well as the Hertzian elastic contact at the same load. The validity of the calculated results, although not shown here, was certified from the relationship between the rolling load and elongation[10]. Considering the characteristics of typical skin-pass rolling conditions, the following observations are recognized. The pressure distribution has its peak around the center of the contact length due to high hydrostatic pressure, or a so-called friction hill. This distribution can be roughly estimated by simple vertical compression. Furthermore, the peak pressure around the center is almost the same as Hertzian elastic contact. Estimation error is negligible up to 1% elongation, which is the typical elongation value in skin-pass rolling operation. This is due to the fact that, considering the characteristics of skin-pass rolling, the sticking region dominates the contact length[16] and the contact length is quite large in comparison with the change in thickness due to the use of a large-diameter work roll. In Fig. 2, for example, the ratio of the contact length over the change in thickness is more than 500 at the elongation of 1%. If the elastic deformation of the work roll is considered, this condition can reasonably be estimated as being Hertzian contact.

3. Roughness Profile Transfer in Dull Skin–Pass Rolling

3.1 Experimental and FEM Conditions Considering Work Roll Surface Roughness

The processing of the work roll surface mentioned in the previous section (R250 in the following figures) to a dull finish by electro-discharge texturing, similar skin-pass rolling and vertical compression experiments

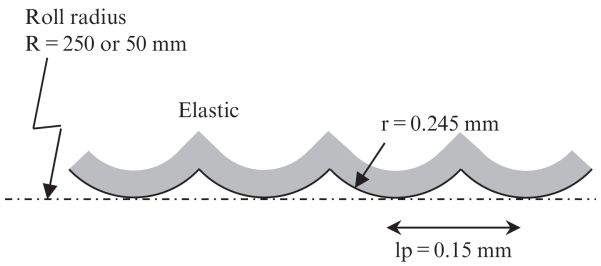

Fig. 3 Roughness profile model of roll surface[12)]

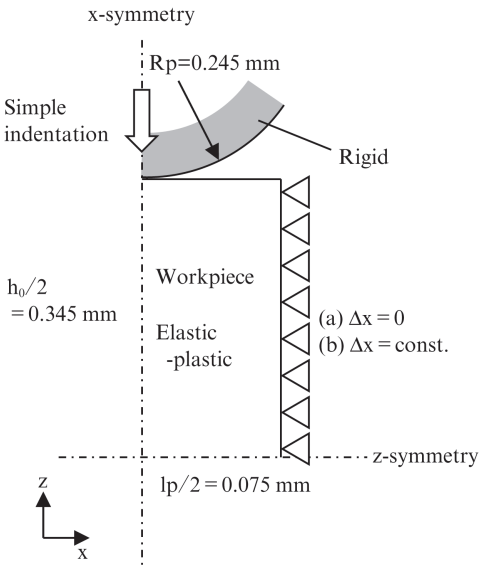

Fig. 4 Schematic outline of vertical indentation model of one roughness profile[12)]

were conducted. The work roll surface was prepared to be 3 μm Ra in the axial direction under the measurement conditions of cut-off of 2.5 mm and measurement length of 12.5 mm. The similar skin-pass rolling experiment was conducted with another laboratory rolling mill with a small work roll of 100 mm diameter (R50 in the following figures) to evaluate the effect of work roll size. After the experiments of skin-pass rolling and simple compression, the surface roughness on the workpiece was measured, and the roughness transfer ratio was calculated by deducting the workpiece surface roughness before the experiment, as expressed in equation (1).

$$\gamma[\%] = 100 \cdot \left(R_{a\_S1} - R_{a\_S0}\right) \Big/ \left(R_{a\_R} - R_{a\_S0}\right) \quad \cdots\cdots (1)$$

where, Ra_S0: workpiece roughness before rolling, Ra_S1: workpiece roughness after rolling and Ra_R: roll roughness. The direction of measurement of the workpiece surface was the transverse direction. For the vertical compression experiment, roughness was measured around the center of the contact area.

To clarify the characteristics of roughness transfer with a large work roll, an FEM analysis of the experimental skin-pass rolling and vertical compression conditions mentioned above was conducted. The surface roughness profile of the work roll was taken into account by modeling the roughness profile as a series of circle segments in the rolling direction, as shown in **Fig. 3** [12)]. The roughness profile radius was decided so that the average roughness of the roughness profile model was 3 μm Ra. The other basic analytical conditions except the roll surface roughness model are the same as in Chapter 2.

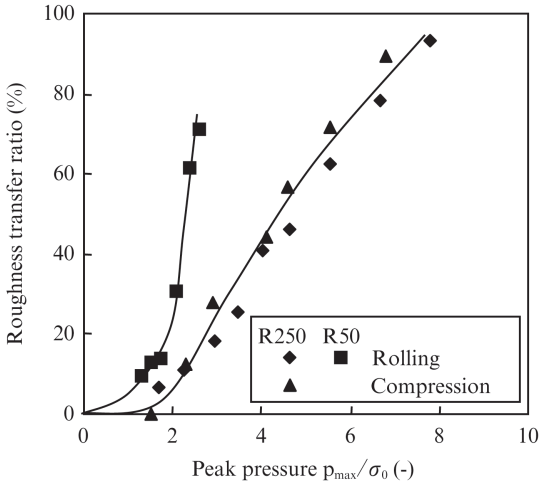

Fig. 5 Roughness transfer ratio by peak pressure[12)]

An additional case of simple vertical indentation of one roughness profile, as shown in **Fig. 4** [12)], was also analyzed, modelling the condition at the peak pressure in the contact length based on the assumption that global deformation of the workpiece is constrained by high hydrostatic pressure. The circular arc in Fig. 4 is not the outer perimeter of the work roll itself. Although the material parameters are the same as in Chapter 2, the circular arc of the roughness profile in Fig. 4 was assumed to be rigid. To model deformation under high hydrostatic pressure, displacement in the x direction was constrained on the free surface on the right hand side in the model to fix the deformation of the bulk.

3.2 Peak Pressure and Roughness Transfer Ratio

Figure 5 [12)] shows the relationship between the roughness transfer in the experiment and the non-dimensional peak pressure over the initial yield stress calculated from the analysis of the skin-pass rolling and vertical compression conditions in Chapter 2. As seen in Fig. 2, the values of peak pressure are almost the same for skin-pass rolling and vertical indentation at the same load. For the large work roll (R250), the skin-pass elongation corresponding to the maximum value of the peak pressure on the abscissa is approximately 2%. Roughness transfer in skin-pass rolling can

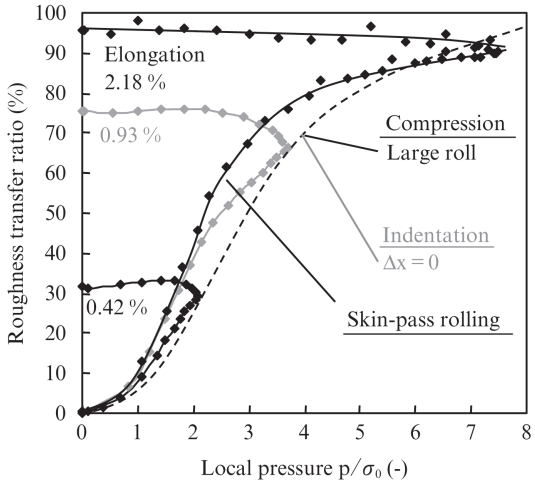

Fig. 6 Calculated relationship between local pressure and roughness transfer, compared with simple compression and indentation[12)]

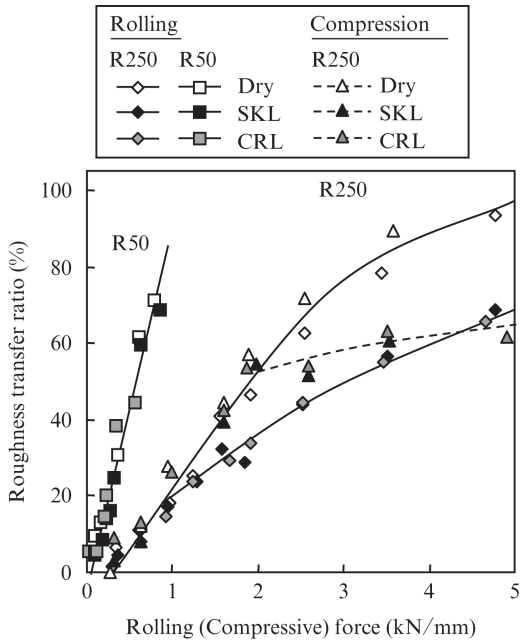

Fig. 7 Relationship of roughness transfer ratio and rolling/compressive force[15)]

be estimated by vertical indentation at the same load in this figure. That is to say, it is strongly implied that the peak pressure is the dominant parameter for roughness transfer in the case of a large roll.

Figure 6 [12)] shows the results of the FEM analyses considering work roll surface roughness. This figure shows the relationship between the local average pressure for one roughness profile in the contact length and the roughness transfer at that profile point in the skin-pass rolling condition. The vertical compression condition and the indentation condition of one roughness profile in Fig. 4 are also drawn with the dashed line. The roughness transfer values for those two conditions almost coincide and are drawn with one line.

In the case of the skin-pass rolling condition, the origin corresponds to the entrance point of the contact length. As rolling progresses, roughness transfer increases along with pressure. The maximum value on the abscissa corresponds to the point of peak pressure, and afterward the pressure decreases moving left on the abscissa and becomes zero, meaning the delivery point of the contact length. The roughness transfer at the peak pressure in the skin-pass rolling condition was in good agreement with the results of vertical compression and simple indentation of the roughness profile. This means that roughness transfer at the peak pressure can be considered to be vertical indentation of the roughness profile in terms of the characteristic of the skin-pass rolling condition, in which a large contact length and sticking region lead to high hydrostatic pressure around the center of the contact length, as revealed in Chapter 2. As a matter of fact, roughness transfer can be organized by peak pressure as shown in Fig. 5, and the peak pressure can be approximated and simplified as Hertzian contact as in Fig. 2.

Although the calculated roughness transfer tends to increase after the peak pressure in Fig. 6, the actual effect is negligible, as can be recognized from Fig. 5. The calculated increase of roughness transfer is due to the relative slide between the work roll and the workpiece in the forward slip region near the delivery point of the contact length, leading to so-called junction-growth. The same tendency was studied in a plane strain upsetting test with small reduction[17, 18)].

As is also obvious from Fig. 5, roughness transfers cannot be quantitatively compared between large and small work roll conditions. The characteristic behavior of roughness transfer in skin-pass rolling is obtained as a result of the long contact length of the large work roll, and thus is difficult to reproduce with a small work roll, which has a small contact length. Rather, qualitative tendencies can be modeled by plane strain upsetting with small reduction of a flat sheet having a similar contact length[17, 18)].

4. Effect of Lubrication on Dull Skin–Pass Rolling

4.1 Experimental Conditions and Evaluation Parameters

The effect of lubrication was investigated in a skin-pass rolling experiment under the same conditions as in Chapter 3. Two types of lubricants were applied; one was a soluble organic acid amine skin-pass rolling lubricant (SKL) with viscosity of 1 mm^2/s at 50°C, and the other was a synthetic ester cold-rolling lubricant

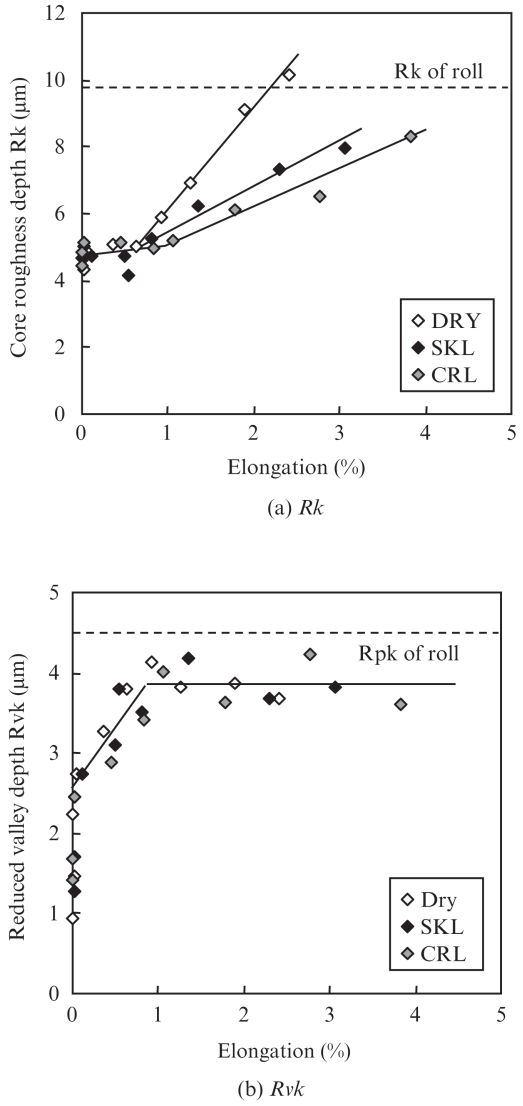

Fig. 8 Relationship of elongation and roughness parameters[15)]

(CRL) with viscosity of 19 mm^2/s at 50°C. The lubricants in the neat condition were applied sufficiently to the workpiece and work roll surfaces with a brush before rolling.

In addition to average roughness (*Ra*), the height characterization parameters of the linear material ratio curve defined in ISO 13565 were also evaluated to clarify quantitatively the effect of lubrication on roughness transfer. The parameters used here were the core roughness depth (*Rk*), which expresses the general tendency of roughness transfer, reduced valley depth (*Rvk*), which expresses the average depth of deep pits on the workpiece surface by indentation from roughness profile peaks on the work roll surface, and reduced peak height (*Rpk*), which expresses the average height of protruding peaks above the roughness core profile toward hollows in the work roll surface roughness profile.

4.2 Experimental Results and Discussion

Figure 7 [15)] shows the relationship between rolling force and the roughness transfer ratio. The transferred roughness was decreased with lubrication above the rolling force of 1 kN/mm, corresponding to elongation of approximately 0.5%. The effect of lubrication differed between the skin-pass rolling and vertical compression conditions. With the small work roll (R50), the tendency did not coincide quantitatively with that of the large work roll (R250), and no effect of lubrication could be observed.

Figure 8 [15)] shows the measured values of *Rk* and *Rvk* after rolling. At a very small elongation, *Rvk* increases rapidly, implying formation of pits on the workpiece surface by indentation from roughness profile peaks, and reaches a constant value at elongation of approximately 1%. In this elongation range, the lubricant escapes into spaces between the roughness profiles, and virtually no effect of lubrication on roughness transfer can be seen. Above this elongation limit, the core roughness profile on the work roll surface is transferred to the workpiece surface, resulting in the increase of *Rk* of the work roll surface. The effect of lubrication appears as the difference in the transfer of the core roughness depth *Rk*. This implies that the lubricant trapped between the roughness profiles disrupts roughness transfer. As a lubricant with larger viscosity is used, the effect becomes more intense. Although not shown here, the results confirmed that no effect of lubrication on *Rpk* could be seen.

As discussed above, the effect of lubrication on elongation and roughness transfer was quite reasonably explained by the height characterization parameters of the linear material ratio curve.

5. Concluding Remarks

In this report, the results of an experimental and analytical investigation of the mechanism of roughness transfer to the workpiece surface in skin-pass rolling were introduced and discussed from the viewpoints of workpiece deformation and lubrication. One of the important characteristics of skin-pass rolling is the use of work rolls having a large diameter compared to the reduction in thickness, resulting in a long contact length with large hydrostatic pressure around the center. Due to this characteristic, the roughness transfer in skin-pass rolling can be modeled as simple vertical compression, and the peak pressure, which is the most important parameter for roughness transfer, can be estimated by Hertzian contact theory. The effect of lubrication is explained clearly and rationally by using the height characterization parameters of the linear

material ratio curve. After the peaks of the roughness profile on the work roll surface are transferred to the workpiece surface under small elongation, lubricants are packed between the surfaces, reducing further roughness transfer. The small-diameter work rolls commonly used in laboratory rolling mills are not appropriate to model the characteristic phenomena in skin-pass rolling in terms of contact length.

Investigation of the above-mentioned mechanism in skin-pass rolling has progressed as it has become possible to consider surface roughness in FEM analyses. Further increases in calculation capacity may enable more complicated analysis, for example, three-dimensional analysis with minimum simplification or premises. Skin-pass rolling is originally a process of rolling steel strips which display the yield point phenomenon. Issues concerning identification of material mechanical properties with the yield point phenomenon and stable calculation of deforming materials with severe work-softening remain to be solved[19]. A detailed numerical investigation of severe inhomogeneous deformation has been conducted with a certain hypothetical material property[20]. Furthermore, more general calculations taking into account detailed work roll elastic deformation as axial bending and flattening could clarify an unknown mechanism for flatness defects[21, 22].

This manuscript is a reedited version of a paper published in the Proceedings of the 320th Symposium on Plastic Processing in The Japan Society for Technology of Plasticity[23].

References

1) Finstermann, G.; Nopp, G.; Eisenköck, N.; Keintzel, G. Proc. 2002 AISE Annual Conventions and Steel Expo. 2002, (CD-ROM).
2) Richter, H. P.; Pawelski, H.; Denker, W.; Holz, R.; Koen, K. Proc. 9th Int. Steel Rolling Conf., ATS, Paris, 2006, vol. 9, p. 198 (Session 14, Paper 5, CD-ROM).
3) Kajiwara, T.; Morimoto, K.; Nakano, T.; Fukuyama, G. Proc. 42nd Jpn. Joint Conf. Technol. Plast. 1991, vol. 42, p. 465.
4) Yarita, I.; Ito, M. Tetsu-to-Hagané. 2008, vol. 94, p. 391.
5) Aoki, I. J. Jpn. Soc. Technol. Plast. 1979, vol. 20, p. 1121.
6) Kato, T. J. Jpn. Soc. Technol. Plast. 1995, vol. 36, p. 332.
7) Kimura, Y.; Ueno, M.; Mihara, Y. Tetsu-to-Hagané. 2009, vol. 95, p. 399.
8) Sun, J.; Huang, H.; Du, F.; Li, X. J. Iron Steel Res. Int. 2009, vol. 16, p. 27.
9) Akashi, T.; Shiraishi, T.; Ogawa, S.; Matsuse, Y. J. Jpn. Soc. Technol. Plast. 2013, vol. 54, p. 606.
10) Kijima, H. J. Mater. Process. Technol. 2013, vol. 213, p. 1764.
11) Akashi, T.; Shiraishi, T.; Ogawa, S.; Matsuse, Y. J. Jpn. Soc. Technol. Plast. 2014, vol. 55, p. 324.
12) Kijima, H. J. Mater. Process. Technol. 2014, vol. 214, p. 1111.
13) Akashi, T.; Shiraishi, T.; Ogawa, S.; Matsuse, Y.; Morihara, H. J. Jpn. Soc. Technol. Plast. 2015, vol. 56, p. 53.
14) Kijima, H. J. Mater. Process. Technol. 2015, vol. 216, p. 1.
15) Kijima, H. J. Mater. Process. Technol. 2015, vol. 225, p. 1.
16) Kijima, H.; Bay, N. CIRP Ann. 2007, vol. 56, p. 301.
17) Kijima, H.; Bay, N. Int. J. Mach. Tools Manuf. 2008, vol. 48, p. 1313.
18) Kijima, H.; Bay, N. Int. J. Mach. Tools Manuf. 2008, vol. 48, p. 1308.
19) Sun, H. B.; Kaneda, Y.; Ohmori, M.; Yoshida, F. Mater. Trans. 2006, vol. 47, p. 96.
20) Giarola, A. M.; Pereira, P. H. R.; Stemler, P. A.; Pertence, A. E. M.; Campos, H. B.; Aguilar, M. T. P.; Cetlin, P. R. J. Mater. Process. Technol. 2015, vol. 216, p. 234.
21) Kijima, H.; Kenmochi, K.; Kitahama, M. J. Jpn. Soc. Technol. Plast. 2002, vol. 43, p. 199.
22) Kijima, H.; Kitahama, M. J. Jpn. Soc. Technol. Plast. 2002, vol. 43, p. 150.
23) Kijima, H. Proc. 320th Symp. Plast. 2016, vol. 320, p. 31.